X-ray-absorption spectroscopy study of the partial devitrification of amorphous $Ni_{80}B_{20}$ and the formation of amorphous nickel

A. Gutiérrez and M. F. López
Centro Nacional de Investigaciones Metalúrgicas (CENIM), CSIC, Av Gregorio del Amo, 8, 28040 Madrid, Spain

A. Hernando
Instituto de Magnetismo Aplicado UCM-RENFE, Las Rozas, Madrid, Spain
and Departamento de Física de Materiales, Universidad Complutense, Madrid, Spain

J. M. Rojo
Departamento de Física de Materiales, Universidad Complutense, Madrid, Spain
(Received 18 March 1997)

The devitrification of initially amorphous $Ni_{80}B_{20}$ has been studied by x-ray-absorption spectroscopy as a function of the annealing temperature. It is found that the full width at half maximum (FWHM) of the main absorption peak at ≈850 eV is sensitive to the degree of amorphization of the specimen. The initial FWHM of 2.51 eV for the homogeneous amorphous $Ni_{80}B_{20}$ decreases to a value of 2.12 eV for the crystalline final mixture of Ni and Ni_3B. In an intermediate, partially devitrified state, a FWHM of 2.30 eV is measured, which supports an earlier identification of pure amorphous nickel. [S0163-1829(97)06634-4]

Amorphous metallic systems are currently the subject of intensive research but many uncertainties still remain when trying to explain some of their remarkable properties in terms of microscopic parameters.[1] Just the existence of amorphous phases in some of these systems is frequently the subject of debate and progress has also been slow in explaining why metals seem to require the presence of a second component, often a metalloid, in order to stabilize amorphous phases.[2] However, some of us have recently proposed that, embedded in a Ni_3B polycrystalline matrix, an amorphous phase of pure nickel can be present at room temperature.[3] This finding opens a way of checking a number of interesting theoretical predictions, for example, in relation to the magnetic properties of such a phase.[4] Although differential scanning calorimetry coupled to x-ray-diffraction data duly has advocated the proposed interpretation, the fact that such an amorphous phase has never previously been observed makes it appropriate to report any additional evidence. In this paper we present an x-ray-absorption spectroscopy (XAS) study of samples similar to those of Ref. 3 and argue that the results are fully consistent with the presence of an amorphous nickel phase along with the crystal matrix.

Samples containing amorphous nickel were prepared according to the procedure discussed in Ref. 3: We shall call state *a* the original all-amorphous homogeneous material prepared by the well-known melt spinning technique from a master alloy of nominal $Ni_{80}B_{20}$ composition. As most of its related alloys, in the limit of high-temperature annealings (for example, 1 h at 750 K), the system devitrifies into a mixture of crystalline Ni_3B and Ni phases, roughly in a 3:1 at. % nickel ratio, which we shall call state *c*. The crucial point is the existence of an intermediate partially devitrified state, that we shall call state *b*, that evolves after an annealing of about 1 h at 600 K, in which the crystallites of Ni_3B have already been formed but the *excess* nickel appears to be in an *amorphous state*. Only after further higher temperature annealing (leading to state *c*) does this excedent nickel crystallize. The main results of the previous investigation are summarized in the third and fourth columns of Table I.

Samples from all three states *a*, *b*, and *c* were prepared, along with a reference specimen of pure crystalline nickel for XAS analysis. After introduction in the ultra-high-vacuum chamber (pressure lower than 5×10^{-10} mbar) the samples were ion sputtered for 10 min with Ar^+ ions of 3 keV in order to remove the surface oxide layer; after this cleaning process the oxygen *K* edge in the x-ray absorption spectra was negligible for all samples. In order to carry on our analysis, nickel L_{III} absorption spectra were recorded in total electron yield mode with an energy resolution that was set to 0.5

TABLE I. Position and full-width at half-maximum of the main nickel L_{III} absorption peak after the data treatment described in the text for (a) sample from state *a*, homogeneous amorphous $Ni_{80}B_{20}$ alloy, (b) sample from state *b*, crystalline Ni_3B plus amorphous Ni, (c) sample from state *c*, a mixture of crystalline Ni_3B and Ni phases, and (d) a reference polycrystalline nickel. In columns 3 and 4 a summary of the main characteristics of samples (a) to (c), as reported in Ref. 3, are also shown.

	Position (eV)	FWHM (eV)	X-ray diffraction (Ref. 3)	Assignment (Ref. 3)
Ni	850.3	1.60	Ni peaks	Crystalline Ni
a	850.3	2.51	No peaks	Amorphous $Ni_{80}B_{20}$
b	850.3	2.30	Ni_3B peaks	Crystal. Ni_3B+ Amorphous Ni
c	850.1	2.12	Ni_3B+Ni peaks	Crystal. Ni_3B+ Crystal. Ni

 © 1997 The American Physical Society

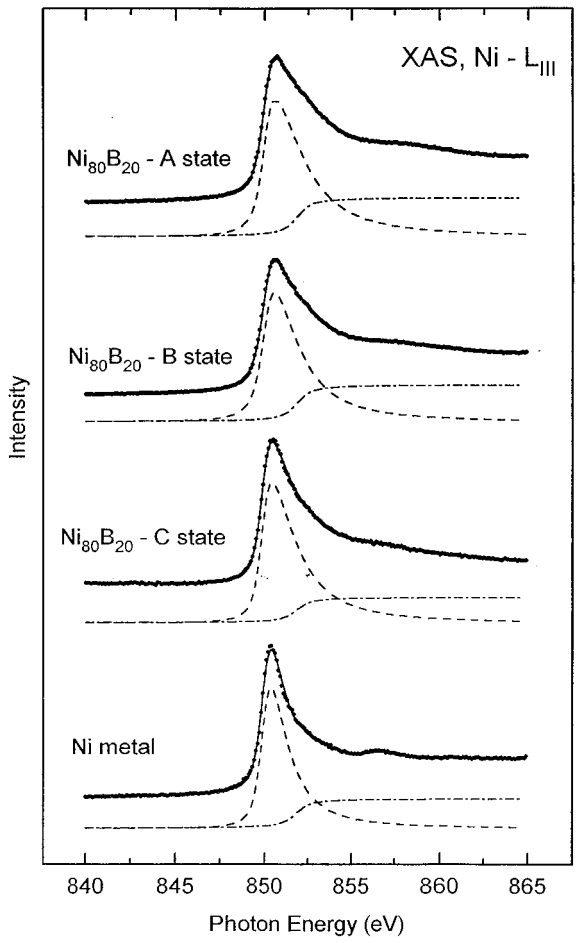

FIG. 1. X-ray-absorption spectra at the nickel L_{III} edge of a $Ni_{80}B_{20}$ alloy in (a) initial amorphous state, (b) partially devitrified state, and (c) totally recrystallized state. A spectrum from crystalline nickel (d) is shown as a reference. The solid line through the data points is the result of a least-squares fitting as described in the text. The dashed line corresponds to the asymmetric Lorentzian component used in the fit and the dashed-dotted line to the arctangent component simulating transitions into the continuum.

eV at a photon energy of ≈850 eV. The data were taken with the SX 700/II monochromator of the Berliner Elektronenspeicherring für Synchrotronstrahlung (BESSY) operated by the Freie Universität Berlin.

In Fig. 1, we show XAS spectra at the nickel L_{III} absorption threshold from the *a*, *b*, and *c* states evolved from the original $Ni_{80}B_{20}$, along with a crystalline nickel reference. The main difference between the four XAS spectra can be traced to the variation of the *width* of the main peak. It is largest for the all-amorphous *a* sample, decreases across *b* as the degree of crystallization increases, and decreases still further in state *c* where the degree of crystallization is maximum. Note that the width is minimum for the reference nickel sample. In order to have a quantitative estimation of the observed behavior, we have carried out a conventional[5] analysis of the absorption data in which a trial function (solid line in the figure) has been fitted to the experimental points by means of a least-squares analysis. The trial function consists of an asymmetric Lorentz line, (dashed component) describing transitions from the Ni-$2p$ core level to discrete $3d$ empty states, plus three corrections: (i) an arctangent (dash-dotted line) describing transitions into the continuum; (ii) an additional Lorentz line (not shown in the figure) to account for the small satellite at ≈857 eV; (iii) a final convolution with a Gauss function to simulate the experimental resolution. The Lorentzian component encompasses the relevant physics of the process and the full width at half maximum (FWHM) σ of all spectra shown in Fig. 1, as well as the energy position of the corresponding Lorentzian peaks, are indicated in the first and second columns of Table I. No comparable analysis has been made in the XAS spectra of boron because, due to the low counting rate, the resolution was poor.

By comparing the FWHM values corresponding to samples *c* and crystalline nickel, it is clear that $\sigma_{Ni3B} > \sigma_{Ni(cr)}$, the latter being the FWHM of crystalline nickel. Also, from a comparison of *b* and *c* one concludes that the value of σ for the excess component of nickel $\sigma_{Ni(ex)}$ in *b* is definitely larger than the corresponding value in crystalline nickel, i.e., $\sigma_{Ni(ex)} > \sigma_{Ni(cr)}$. This shows that the excess nickel in state *b* is not in the normal crystal phase and is most likely disordered. Assuming true Lorentzian peaks, one can make use of the additiveness of Lorentzian widths[6] and assign absolute values to the FWHM of the individual components in the mixtures corresponding to the samples *b* and *c*. From the data of Table I, assuming a 3:1 ratio for the Ni concentrations in Ni_3B and Ni (either crystalline in *c* or amorphous in *b*) we immediately obtain intrinsic FWHM's for the two phases: $\sigma_{Ni3B} = 2.29$ eV, $\sigma_{Ni(ex)} = 2.33$ eV. The latter value is definitely higher than the one corresponding to crystalline nickel $\sigma_{Ni(cry)} = 1.60$ eV, and clearly supports our previous proposal[3] that nickel in state *b* is actually amorphous.

The line shape of the absorption spectra is frequently approximated to the density of unoccupied states. Whereas this approach is valid at the *K* edge in transition metals, where single particle schemes can be used, at the *L* edge the interaction between the excited $3d$ electron and the $2p$ hole leads to a final state multiplet.[7] In the latter case, the spectral line shape can be quite complicated and extremely sensitive to the atomic environment since the local crystal field implies an important perturbation to the intraatomic interactions.[8] In the amorphous phase, a broadening of the absorption spectrum is expected as a result of the enlarged distribution of neighboring atoms, which results in a high dispersion of crystal field values at the absorbing site. This is certainly supported by our raw data in Table I in which the all-amorphous sample (state *a*) has the largest width of the series. Notice, in passing, that the broadening occurs only at the high-energy side of the spectrum since the low-energy side (or absorption edge) is limited by the Fermi edge. We tentatively propose that the width increase in the nickel FWHM from state *c* to *b*, $\sigma_{Ni(ex)} - \sigma_{(cry)} = 0.73$ eV, is due to the presence of an amorphous pure nickel phase in *b*. In this amorphous phase, there is a smeared distribution of neighbor distances and angles that results in broadening of the absorption peak.

In summary, XAS has been used to characterize the different states resulting from the controlled devitrification of an initially homogeneous amorphous alloy $Ni_{80}B_{20}$. An intermediate, partially devitrified state is observed in which the nickel component has a FWHM about 50% larger than the

one corresponding to crystalline nickel. These XAS measurements support a previous x-ray-diffraction interpretation of that component as an amorphous phase of nickel at room temperature.

We are indebted to M. El-Ghannami for supplying us with the specimens. This work has been partially supported by BESSY-EU Project No. CHGE-CT93-0027 of the Human Capital and Mobility programme of the European Union.

[1] *Rapidly Solidified Alloys*, edited by H. H. Liebermann (Dekker, New York, 1993).

[2] T. Egami and Y. Waseda, J. Non-Cryst. Solids **64**, 113 (1984).

[3] J. M. Rojo, A. Hernando, M. El-Ghannami, A. García-Escorial, M. A. González, R. García-Martínez, and L. Ricciarelli, Phys. Rev. Lett. **76**, 4833 (1996).

[4] A. Posada-Amarillas and I. L. Garzón, Phys. Rev. B **53**, 8363 (1996); B. Szpunar, U. Erb, G. Palumbo, K. T. Aust, and L. J. Lewis, *ibid*. **53**, 5547 (1996); M. Liebs, K. Hummler, and M. Fähnle, *ibid*. **51**, 8664 (1995).

[5] Z. Hu, G. Kaindl, D. Vandré, R. Hoppe, and G. Wortmann, J. Alloys Compd. **205**, 263 (1994); A. Gutiérrez, J. Díaz, and M. F. López, Appl. Phys. A **61**, 111 (1995).

[6] See, for example, R. London, *The Quantum Theory of Light* (Oxford University Press, Oxford, 1983), pp. 74–78.

[7] F. M. F. de Groot, J. Electron Spectrosc. Relat. Phenom. **67**, 529 (1994).

[8] F. M. F. de Groot, J. C. Fuggle, B. T. Thole, and G. A. Sawatzky, Phys. Rev. B **42**, 5459 (1990).